Atmospheric
Chemistry
and Physics
Discussions

Open Access

Factors that influence surface PM$_{2.5}$ values inferred from satellite observations: perspective gained for the Baltimore-Washington Area during DISCOVER-AQ

S. Crumeyrolle, G. Chen, L. Ziemba, A. Beyersdorf, L. Thornhill, E. Winstead, R. Moore, M. A. Shook, and B. Anderson

NASA Langley Research Center, Hampton, VA 23666, USA

Correspondence to: S. Crumeyrolle (suzanne.crumeyrolle@gmail.com)

ACPD

13, 23421–23459, 2013

PM$_{2.5}$ values inferred from satellite observations

S. Crumeyrolle et al.

Title Page

Abstract | Introduction

Conclusions | References

Tables | Figures

|◄ | ►|

◄ | ►

Back | Close

Full Screen / Esc

Printer-friendly Version

Interactive Discussion

Abstract

During the NASA DISCOVER-AQ campaign over the Washington D.C., - Baltimore, MD, metropolitan region in July 2011, the NASA P-3B aircraft performed extensive profiling of aerosol optical, chemical, and microphysical properties. These in-situ profiles were coincident with ground based remote sensing (AERONET) and in-situ ($PM_{2.5}$) measurements. Here, we use this data set to study the correlation between the $PM_{2.5}$ observations at the surface and the column integrated measurements. Aerosol optical depth (AOD) calculated with the extinction (532 nm) measured during the in-situ profiles was found to be strongly correlated with the volume of aerosols present in the boundary layer (BL). Despite the strong correlation, some variability remains, and we find that the presence of aerosol layers above the BL (in the buffer layer – BuL) introduces a significant uncertainties in $PM_{2.5}$ estimates based on column-integrated measurements. This motivates the use of active remote sensing techniques to dramatically improve air quality retrievals. Since more than a quarter of the AOD values observed during DISCOVER-AQ are dominated by aerosol water uptake, the $f(RH)_{amb}$ (obtained from two nephelometers at different relative humidities – RHs) is used to study the impact of the aerosol hygroscopicity. The results indicate that $PM_{2.5}$ can be predicted within a factor of 1.6 even when the vertical variability of the $f(RH)_{amb}$ is assumed to be negligible.

1 Introduction

Atmospheric aerosol particles have important influences on global climate and ecosystem processes depending on their physical and chemical properties. Due to numerous studies highlighting negative health effects as a result of aerosol particle exposure, more efficient abatement measures have received serious consideration (Annesi-Maesano et al., 2007). Particulate matter (PM) is classified as a criteria pollutant and air quality standards have been established addressing $PM_{2.5}$, which represents the

total mass concentration of particles with aerodynamic diameters less than 2.5 µm. The current air quality monitoring network provides relatively sparse geographic coverage and is mostly limited to urban areas where $PM_{2.5}$ concentrations are greatest. Improving global air quality monitoring measurement resolution to capture small-scale variability is a necessary priority of both the scientific and policy communities.

One important step toward this goal is the use of spaceborne sensors that allow near-continuous aerosol monitoring throughout the world. Yet, the complexity and resolution of aerosol satellite retrievals, as well as uncertainties associated with cloud interference, challenge these efforts. Several studies have explored the possibility of evaluating air quality from space (Hoff and Christopher, 2009 and references therein) and report comparisons between space and ground level measurements of aerosol concentrations for Europe (Chu et al., 2003; Vidot et al., 2007; Schaap et al., 2009), Canada (Van Donkelaar et al., 2006), the United States (Wang and Christopher, 2003; Engel Cox et al., 2004; Van Donkelaar et al., 2006; Gupta and Christopher, 2009), and other locations around the globe (Gupta et al., 2007; Kumar et al., 2007, 2008). Overall, these studies have attempted to relate the spaceborne column measurements of aerosol optical attenuation to surface measurements of $PM_{2.5}$, especially in the summertime (Engel-Cox et al., 2006; Tian and Chen, 2010) and over urban areas (Liu et al., 2005; Schaap et al., 2009). The eastern United States has been shown to be a good location for ascertaining $PM_{2.5}$ information from aerosol optical depth (AOD) due to (1) more uniform vertical distribution of aerosols, (2) chemical composition that is dominated by sulfates, (3) a uniform topography and (4) widely distributed anthropogenic emission sources (Engel-Cox et al., 2006).

However, the uncertainty in relating a column integrated AOD to ground-level $PM_{2.5}$ is compounded by timing mismatches between the measurements. Ground measurements necessitate averaging over time-scales from hourly to daily, which improves the $PM_{2.5}$/AOD relationship (Gupta et al., 2006) but sacrifices accuracy during strong, short-lived pollution events that may be critical for air quality predictions and assessing air quality non-attainment. In addition, surface reflections (i.e., albedo) can complicate

PM$_{2.5}$ values inferred from satellite observations

S. Crumeyrolle et al.

Full Screen / Esc

Printer-friendly Version

Interactive Discussion

spaceborne AOD measurements resulting in seasonal and ground-cover bias. For example, retrievals over desert regions or snow-covered areas during the winter season can lead to the overestimation of the AOD (Van Donkelaar et al., 2006) and therefore an overestimate in PM$_{2.5}$.

Recent field work over the United-States (Al-Saadi et al., 2008) and a three-year analysis in Taiwan (Tsai et al., 2011) using airborne (high-spectral resolution lidar, HSRL) and ground-based lidar measurements (micro-pulse lidar network (MPLnet) or aerosol robotic network (AERONET)) suggest vertical distributions are helpful to normalize satellite observations of column AOD and result in dramatically improved correlation with surface PM$_{2.5}$ observations. Although incorporating the boundary layer (BL) depth improves the AOD- PM$_{2.5}$ relationship, elevated layers can still confound results. Several studies reported the importance of an aerosol layer above the BL since elevated aerosol layers increase the AOD but are decoupled from the surface based extinction measurements (Engel-Cox et al., 2006; Schafer et al., 2008; He et al., 2008). He et al. (2008) found that only 64 % of the monthly mean aerosol optical depth over Hong Kong is due to aerosols in the BL. Still, while lidar measurements have shown a promising path forward, the limited spatial and temporal coverage of current measurements make assumptions necessary to extrapolate vertical distributions over regional and global scales.

A major advantage of remote sensing techniques is that they give information about particles as they occur in the atmosphere (i.e., at ambient relative humidity (RH)), while in-situ aerosol measurements, including PM$_{2.5}$, are generally performed at drier conditions (often RH $\leq$ 50 %, Collaud Coen et al., 2013). The amount of water absorbed by an aerosol is a function of its dry diameter and chemical composition. This changes the ambient aerosol mass (Pilinis and Seinfeld, 1989) and the aerosol optical properties (Schuster et al., 2009) and thus the AOD (Koelemeijer et al., 2006). Currently, aerosol liquid water content is not measured at the ground sites of the global atmosphere watch (GAW) network and nor at a global scale, so many studies either neglect the aerosol liquid water content when parameterizing the relationship between AOD and PM$_{2.5}$

(Kaufman et al., 2002; Liu et al., 2005; Kumar et al., 2007; Schaap et al., 2009) or use an empirically-derived dependence of extinction coefficient on relative humidity f(RH) and the surface ambient RH to estimate the aerosol liquid water content throughout the atmospheric column (e.g., Tsai et al., 2011; Koelemeijer et al., 2006). Gupta and Christopher (2009a) showed that the inclusion of meteorological parameters (e.g., RH, temperature, wind speed and cloud fraction) in addition to the BL height improved the estimation of ground level PM$_{2.5}$ from column-integrated measurement by 21 %.

Given the possible benefits and current challenges of utilizing satellite-based observations to predict ground-level particulate air quality, the NASA DISCOVER-AQ (Deriving Information on Surface Conditions from COlumn and VERtically Resolved Observations Relevant to Air Quality) project was designed to deploy a coordinated and complex suite of ground and airborne measurements. The DISCOVER-AQ strategy is to make systematic, co-located observations of aerosol properties by in-situ and remote-sensing techniques over geographically complex source regions (Washington, D.C. in Summer-2011, the San Juaquin Valley of California in Winter-2013, and the Houston, TX in Summer-2013) and over surface-based monitoring stations to provide continuous measurements of criteria pollutants. Here we focus on the Washington D.C. campaign and use this dataset to evaluate our ability to diagnose surface PM$_{2.5}$ conditions from simulated satellite observations with the unique benefit of a highly systematic characterization of the vertical extent of aerosols along with a dense coverage of ground measurements. The sampling location and the platforms used are described in Sect. 2, the P-3B instrumentation and the observations are described in Sect. 3 and the methodology in Sect. 4. In Sect. 5, the AOD- PM$_{2.5}$ relationship is quantitatively assessed by systematically showing that (i) low-altitude airborne and ground-level measurements can be statistically compared, (ii) changes in ground-level PM$_{2.5}$ (i.e., mass loading, effective radius, and chemical composition) directly affect observed AOD variability, and (iii) knowledge of aerosol vertical distribution and RH are essential parameters to better constrain the derived AOD/PM$_{2.5}$ relationship.

2 Sampling location and platforms

The success of DISCOVER-AQ relies on the systematic and concurrent observation of column-integrated, surface, and vertically-resolved distributions of aerosols and trace gases relevant to air quality as they evolve throughout the day. This has been accomplished with a combination of two NASA aircraft, a P-3B and UC-12, sampling in coordination with surface networks during field campaigns over regions characterized by a wide variety of aerosol sources. This analysis focuses on measurements from the P-3B, which was equipped with in-situ aerosol instruments to measure microphysical, optical, and chemical properties of aerosols. The NASA P-3B aircraft performed 14 flights of nominal 8-hours duration in the Washington, D.C./Baltimore, MD, area in July 2011.

Flight paths for the P-3B varied minimally from flight-to-flight, with each flight normally involving 2 to 4 vertical profiles (spirals) over each ground site (Fig. 1). The large statistical dataset allows unbiased analysis of day-to-day, diurnal, spatial, and vertical variability in this region. The P-3B performed a total of 247 profiles over the six ground sites (43 over Beltsville, 39 over Padonia, 43 over Aldino, 38 over Fairhill, 45 over Edgewood, and 39 over Essex; see Fig. 1 for locations). The range of vertical profile sampling was mostly limited by the air traffic control restrictions. As a result, the vertical profiles are typically from 0.3 to 3.2 km (pressure altitude), except Beltsville, where the top of the profile is about 1.5 km.

3 Instrumentation and observations

3.1 Ground sites

The ground sites were equipped with sun-photometers within the Aerosol Robotic Network (AERONET, Holben et al., 1998) providing a direct measure of AOD at seven wavelengths (approximately 0.340, 0.380, 0.440, 0.500, 0.675, 0.870, and 1.02 µm)

with an estimated uncertainty of 1–2 % (Holben et al., 2001). Beltsville, Fairhill and Edgewood were also equipped with in-situ aerosol and trace gas monitors that were operated within EPA's AQS network (http://www.epa.gov/ttn/airs/airsaqs/). The PM$_{2.5}$ mass concentrations were measured with Met One 1020 beta attenuation monitors (BAM, Macias and Husar, 1976). The PM$_{2.5}$ data are reported as hourly averages. The detection limit for the hourly averaged measurements is reported by the manufacturer at 4.0 µg m^{-3}, and the relative uncertainty is about ±0.1 µg m^{-3}. Ozone mixing ratios were measured at each ground site by UV-absorption (Gao, 2012).

3.2 Airborne (P-3B)

Aerosols were sampled through an isokinetically-controlled inlet and delivered to a comprehensive suite of aerosol instruments on-board the NASA P-3B aircraft. The inlet has been previously evaluated and shown to efficiently transmit particles smaller than 4 µm diameter (McNaughton et al., 2007). Simultaneous measurements of scattering (σ_{scat}) and absorption coefficients (σ_{abs}), aerosol size distribution, and aerosol chemical composition were made during DISCOVER-AQ. Dry scattering coefficient (σ_{scat}) measurements were made at 1 Hz using a three wavelength nephelometer (TSI 3563) operating at 450, 550, and 700 nm at RH less than 40 %. The nephelometer was calibrated using filtered air and CO_2 (Anderson and Ogren, 1998) prior to, during, and after the mission. The scattering coefficient has been corrected from angular truncation errors based on Anderson and Ogren (1998). Measurements σ_{abs} were also at 1 Hz by a Particle Soot Absorption Photometer (PSAP, Radiance Research, Inc.) at 470, 532, and 660 nm wavelengths and interpolated to 550 nm using the observed Angstrom exponent of absorption between 470 and 660 nm. PSAP data have a known scattering interference from particles deposited on the collection filter, and the measurements were post-corrected following Virkkula et al. (2010). The standard corrections on the PSAP measurements limit the accuracy of the measured absorption coefficient to 20 to 30 % (Ryder et al., 2013). Extinction coefficients were then calculated at dry RH (< 40 %) by summing the σ_{scat} and σ_{abs}.

PM$_{2.5}$ values inferred from satellite observations

S. Crumeyrolle et al.

Title Page

Abstract | Introduction

Conclusions | References

Tables | Figures

◄ | ►

◄ | ►

Back | Close

Full Screen / Esc

Printer-friendly Version

Interactive Discussion

Observations of particle hygroscopicity f(RH), defined as the ratio of humidified to dry σ_{scat} were obtained using an additional, parallel three-wavelength integrating nephelometer operating at a RH controlled at 80 ± 4 %. This technique is described in more detail by Ziemba et al. (2013). The sample flow routed to both nephelometers was actively dried using a nafion dryer (Perma-Pure FC-125-240-10PP) which efficiently passed accumulation mode aerosol (> 90 % transmission). Data contaminated by cloud penetrations (droplet shattering on the inlet tip) were identified visually via high particle number concentration and removed. The f(RH)$_{amb}$ used to convert the measured extinction coefficient from dry ($\sigma_{ext,dry}$) to the ambient humidity conditions ($\sigma_{ext,amb}$) is defined as :

$$f\mathrm{RH}_{amb} = \frac{\sigma_{ext,amb}}{\sigma_{ext,dry}} = \left[\frac{1 - \frac{\mathrm{RH}_{amb}}{100}}{1 - \frac{\mathrm{RH}_{dry}}{100}}\right]^{(-\gamma)} \;;\; \gamma = \frac{\ln\left[\frac{\sigma_{scat,wet}}{\sigma_{scat,dry}}\right]}{\ln\left[\frac{100 - \mathrm{RH}_{dry}}{100 - \mathrm{RH}_{wet}}\right]} \tag{1}$$

where γ is an experimentally-determined variable dependent on the dry and wet scattering coefficient ($\sigma_{sca,dry}$ and $\sigma_{sca,wet}$ respectively). During DISCOVER-AQ, γ varied between 0.2 and 0.6, and was inversely correlated with the organic mass fraction of the aerosol (Beyersdorf et al., 2013).

Recently, Ziemba et al. (2013) presented a statistical comparison of in-situ extinction coefficient measurements coincident with remote-sensing observations performed by the HSRL (both measurements were performed at 532 nm). It revealed good agreement (slope 1.11 and $R^2 = 0.88$) consistently over the entire ambient RH range within instrumental uncertainty. Part of this systematic difference may be due to particle losses through the inlet and the dryer (10 % losses through the dryer). This result demonstrated that (1) all the particles observed by the HSRL are within the sampling size range of the in-situ measurements (i.e. particles observed in this region are smaller than the inlet cut-off diameter of 4 µm) and (2) the Gasso parameterisation (Eq. 1) is valid to correct observations performed at dry RH to ambient conditions.

Along with the optical measurements, dry aerosol size distributions were determined for 0.06-1.0 µm diameter particles using a ultra-high sensitivity aerosol spectrometer (UHSAS, Droplet Measurement Technologies) with a 1 Hz frequency. The UHSAS was calibrated with polystyrene latex spheres (PSL) and post-corrected with ammonium
5 sulfate in order to provide optical particle sizing most representative of ambient aerosol. The $\sigma_{\text{scat,dry}}$ measurements were compared to modeled $\sigma_{\text{scat,dry}}$ calculated using Mie theory, the UHSAS size distribution measurements, and assuming a particle refractive index of 1.53 – 0.00 i for ammonium sulfate (Ziemba et al., 2013). This closure exercise (slope of 0.991 ± 0.004 and R^2 of 0.98) gives confidence in both the $\sigma_{\text{scat,dry}}$ and dry
10 size distribution measurements.

Chemical composition measurements were made with a single particle soot photometer (SP2, Droplet Measurement Technologies) and a pair of particle-into-liquid samplers (PILS). The SP2 provides mass-based black carbon particle size distributions by measuring laser-induced incandescence and is calibrated using monodisperse
15 aquadag particles generated with a nebulizer and differential mobility analyzer. The PILS captures soluble aerosol constitutents in the sampled air flow into a liquid flow of deionized water. The first PILS was coupled to a total organic carbon (TOC) analyzer (Sievers Model 800) to give the mass of the water-soluble organic carbon at a 10 s time resolution. The effluent from the second PILS was collected in 0.8 mL vials for
20 later ion chromatographic measurement of sodium, ammonium, potassium, calcium, magnesium, chloride, nitrite, nitrate and sulfate. Sampling intervals for the inorganic analysis varied between three and five minutes.

4 Methodology

The AOD represents the integral of the ambient aerosol extinction coefficient, $\sigma_{ext,amb}$ from the surface (z_{surf}) to the top of the atmosphere (z_{TOA}):

$$AOD = \int_{z_{surf}}^{z_{TOA}} \sigma_{ext,amb}(z)\,dz \tag{2}$$

Since the P-3B profile typically begins at ~ 300 m altitude, it is necessary to add the aerosol extinction between 0–300 m in order to calculate an AOD from the observed $\sigma_{ext,amb}$ (Eq. 2) for comparison with surface-base measurements. In the absence of additional aerosol sources and assuming the boundary layer is well mixed, the measurements between the aircraft and the surface should be coupled and consistent. As the P-3B measurements were performed during the summer, the BL is expected to be well mixed throughout the day time except in the early morning before surface heating becomes a driving factor. The ozone mixing ratio is the only quasi-conserved parameter between the P-3B that is also measured at each of the ground sites and is a good tracer, as it will be fairly uniform in a well-mixed boundary layer. Figure 2 shows the ozone measured at the lowest level of the P-3B profile as a function of ozone at the surface (MDE ground sites). The high correlation coefficient (0.98) and linear regression slope of 1.01 illustrate that mixing in the BL is sufficient to assume aerosol loading and properties are homogeneous from the lowest aircraft altitude to surface. Similar results were obtained for analysis of each site independently. Thus, the AOD_{P-3B} is calculated by assuming a constant σ_{ext}, dry value between the lowest aircraft altitude to surface. The estimated portion is typically less than 16 % of the AOD_{P-3B} and any variability resulting from the assumption of constant aerosol extinction in the surface layer is likely minor.

To evaluate whether the measured AOD_{P-3B} are representative of the entire atmospheric column, values were directly compared to the AOD measured by the

AERONET sun photometers (AOD_{TOA}, see Fig. 3), which is considered a reference for AOD measurements (Holben et al., 1998). Only profiles performed within a one hour window of the AERONET retrievals were used in this comparison. A total of 114 profiles met these criteria. The comparison shows good correlation ($R^2 = 0.96$ for each

5   wavelength), although AOD_{TOA} values are higher than the AOD_{P-3B} by nearly a factor of 1.23, based on the slope of the linear regression. Other studies have also noted that AODs calculated from in-situ instrumentation and retrieved by remote sensing are well correlated, with the latter typically greater than the former (Schmid et al., 2000, 2009; Hartley et al., 2000; Sheridan et al., 2002; Andrews et al., 2004). The larger

10   offset (23 %), compared to the 11 % offset calculated by comparing AOD_{HSRL} and AOD_{P-3B} mostly due to inlet and dryer particle losses, may be due the presence of an aerosol layer above the HSRL flight level (above 8.5 km), incorect AERONET AOD cloud screening, or underestimation of the contribution below the P-3B profile height (closest to the surface).

15   The impact of atmospheric structure on measured AODs was examined using the temperature, relative humidity, and wind data recorded during the P-3B profiles. At least three dynamical layers are evident: the Boundary Layer (BL), the Buffer Layer (BuL) and the Free Troposphere (FT). The well-mixed, boundary layer is determined as Lenschow et al. (1999), while the BuL is the transition layer between the BL and the

20   FT with a pronounced gradient of aerosol concentrations from the typically higher concentration observed in the BL and typically cleaner conditions observed in the FT. The use of the BuL here emphasizes its differences from previous concepts of a residual or intermediate layer. Since the BuL is intermittently turbulent, it can entrain fluid from both the underlying BL and the overlying FT (Russell et al., 1998). Therefore, Eq. (2)

25   can be rewritten to assess the observed AOD:

$$AOD_{P-3B} = \int_{z_{surf}}^{z_{BL}} \sigma_{ext,amb}(z)\,dz + \int_{z_{BL}}^{z_{BuL}} \sigma_{ext,amb}(z)\,dz + \int_{z_{BuL}}^{z_{P-3B}} \sigma_{ext,amb}(z)\,d \qquad (3)$$

where Z_{BL}, Z_{BuL}, and Z_{P-3B} denote the atmospheric boundary layer (BL) height, buffer layer (BuL) top, and the top of the P-3B sampling height, respectively. Each integral of the Eq. (3) reflects the variation of the observed $\sigma_{ext,amb}$ as a function of the altitude, which is shown in Fig. 4a, b, c. These case studies, performed on the 20 July 2011 (a), 21 July 2011 (b) and on the 28 July 2011 (c), represent the three vertical aerosol distributions commonly observed during the campaign. The first study case on the 20 July 2011 (Fig. 4a) represents more than 60 % of observations and highlights high values of $\sigma_{ext,amb}$ within the BL accounting for 62 % of the AOD_{P-3B} (Table 1). The second study case on 21 July 2011 (Fig. 4b), represents 17 % of the observed profiles and shows the presence of the aerosol caped by the top of the BuL. The aerosol present in the BuL accounts for 48 % of AOD_{P-3B} compared to 46 % within the BL (Table 1). Finally, an aerosol layer with significant $\sigma_{ext,amb}$ values can be detected above the buffer layer contributing to 37 % of AOD_{P-3B} (twice the contribution from the BL, Table 1) as observed on the 28 July 2011 (Fig. 4c). The presence of an aerosol layer accounting for a large part of the AOD has been observed in 23 % of the profiles.

Alternatively, $\sigma_{ext,dry}$ (z) can be expressed as the product of the mass extinction efficiency (MEE_{dry}) and aerosol mass loading (M_{dry}) as:

$$\sigma_{ext,dry} = MEE_{dry} \cdot M_{dry} \tag{4}$$

Furthermore, the value of $\sigma_{ext,dry}$ has an averaged small variability within the BL ($< 9\%$). Thus, it is reasonable to believe that the BL is vertically well mixed and assuming that aerosol loading above the BL is negligible, Eq. (3) can be further reduced to Eq. (5), which is commonly cited in literature (Koelemeijer et al., 2006).

$$PM_{2.5} = \frac{\overline{fRH_{amb}}MEE_{dry,surf}z_{BL}}{AOD_{P-3B}} \tag{5}$$

The large number of profiles acquired during the DISCOVER-AQ campaign offers an unique opportunity to study the validity and the impact of the assumptions made in Eq. (5).

5 Results

During the campaign, the $PM_{2.5}$ observations performed at each of the three relevant ground sites show similar temporal tendencies. A time-series for $PM_{2.5}$ at the Edgewood site is shown in Fig. 4d along with the AOD_{P-3B}, the derived mass extinction efficiency (MEE), and the sulfate-to-WSOC (water soluble organic carbon) as a function of the Julian day. This time serie highlights the large variability of the hourly averaged $PM_{2.5}$ within a highly polluted period (Julian Day 201–205, $PM_{2.5}$ greater than $30\,\mu g\,m^{-3}$) and a clean period (Julian Day 195–199, $PM_{2.5}$ less than $10\,\mu g\,m^{-3}$). Note the largest $PM_{2.5}$ values are associated with the highest sulfate/WSOC ratio and the largest effective radius (calculated as the ratio of 3rd and 2nd moments of the UHSAS aerosol size distribution, Fig. 5). In order to determine the geographical origins and the history of these air masses, backtrajectory calculations are performed using the HYSPLIT model (Draxler and Rolph, 2010). HYSPLIT was initialized for each ground site for every P-3B profile four days backward in time. The back trajectories showed that the highly polluted periods were associated with air masses coming from the Ohio River valley, a region typically associated with power plant emissions. Indeed, Peltier et al. (2007) reported sulfate concentration up to $30\,\mu g\,m^{-3}$ over this region during the New England Air Quality Study (NEAQS) airborne field campaign in 2002 and Ziemba et al. (2007) found enhanced ammonium sulfate concentrations associated with long-range transport events from this region to the Northeast United States during ICARTT in 2004. The differences in the aerosol sources may also explain the effective radius differences, as emissions of primary organic aerosol are typically of smaller diameter (Zhang et al., 2005; Volkamer et al., 2006).

The aerosol chemical composition is strongly linked with the aerosol size distribution with larger particles being enriched with sulfate. The aerosol MEE, sensitive to both aerosol physical and chemical properties, was calculated using the $PM_{2.5}$ and the average aerosol extinction measured at the lowest P-3B flight altitude. The MEE varied between 2.6 and $9.7\,m^2\,g^{-1}$ during the entire campaign with a median of $5.04\,m^2\,g^{-1}$. The

highest MEE values correspond to $PM_{2.5}$ values close to the detection limit ($< 4\,\mu g\,m^{-3}$). By filtering the MEE as a function of the sulfate concentration, two distinct aerosol MEEs are observed during the DISCOVER-AQ campaign: aerosols enriched in sulfate related to power plant emissions (MEE $\sim 5.3 \pm 0.4\,m^2\,g^{-1}$) and aerosols enriched in organics related to urban emission (MEE $\sim 3.8 \pm 0.9\,m^2\,g^{-1}$). These values are consistent with previous studies. Husar et al. (2000) reported MEE values measured on the east coast of the United States on average about $4.9\,m^2\,g^{-1}$). Moreover, Pereira et al. (2008) measured the MEE values of anthropogenic pollution present over Portugal in 2006 and observed values around $3\,m^2\,g^{-1}$, while Feczkó et al. (2002) measured the MEE of ammonium sulfate, $(NH_4)_2SO_4$, to be $6\,m^2\,g^{-1}$).

Figure 5 shows the correlation between $PM_{2.5}$ measured from the EPA ground sites at (a) Beltsville, (b) Fairhill, and (c) Edgewood and the $AOD_{P\text{-}3B}$ calculated for each profile performed by the P-3B. The color code corresponds to the effective radius. As previously stated, the profiles performed over Beltsville were confined to altitudes lower than 1.5 km while those performed over Fairhill and Edgewood reached 3 km. The integration of the extinction coefficient over a different altitude range may have cause an underestimation of the AOD over Beltsville. An orthogonal distance regression has been applied for each site for all data (regardless of particle effective radius) and is displayed on the top left corner of each figure. Correlations between integrated column and surface measurements are very strong (correlation coefficients larger than 0.84 at Beltsville, 0.79 at Fairhill and 0.82 at Edgewood). The slopes are similar for each site, 66.1 ($\mu g\,m^{-3}$ per unit of AOD) at Beltsville, 48.5 at Fairhill, and 38.7 at Edgewood. Hoff and Christopher (2009) summarized the linear regressions between the AOD and the $PM_{2.5}$ obtained over the United-States, Europe and China from 15 independent studies. They found the average slope, calculated using only the studies over the United States, was approximately 63 ± 51. Moreover, Engel-Cox et al. (2006) retrieved a slope between 31 and 49 over Baltimore during the summer 2004, which is in good agreement to the values obtained in this study.

Hoff and Christopher (2009) discussed a hypothetical, non-linearity between AOD and PM$_{2.5}$ based on simulation results (Liu et al., 2005) and assumed that this hypothetical non-linearity would be due to a sparse distribution of the AOD values during clean periods (especially for AOD < 0.1). As more than 40 % of the P-3B profiles were
5 performed during clean periods, DISCOVER-AQ offers a great opportunity to study this non-linearity. According to Fig. 5, these clean periods are related to the presence of small particles ($75 < D_p < 100$ nm) enriched in organics (MEE ~ 4 m^2 g^{-1}) in contrast to polluted periods dominated by larger (D_p greater than 100 nm) sulfate particles. According to the Mie theory, small particles (D_p less than 100 nm) are significantly less
10 optically active than larger paricles, but still impact the total aerosol mass. Therefore, the presence of small particles induces non-linearity between the AOD and the PM$_{2.5}$, which is clearly depicted by the linear fits (blue lines) using exclusively the clean periods shown in Fig. 5 for each site. The slopes differ by a factor between 2.5 and 3 and highlight the low extinction efficiency of the small particles ($75 < D_p < 100$ nm);
15 values of 177, 154, 108 µg m^{-3} per unit of AOD were derived for Beltsville, Fairhill, and Edgewood, respectively. Therefore, these results show the necessity of measurements at multiple wavelengths, i.e., determination of the Angstrom Exponent, to account for the non-linearities in the PM$_{2.5}$-AOD relationship due to the presence of small particles. Indeed, the non-linearity can be avoided using a threshold value for the angstrom
20 exponent (less than 2.4).

5.1 Factors affecting the relationship between AOD and PM$_{2.5}$

5.1.1 Aerosol vertical distribution

Using the meteorological parameters measured during the P-3B profiles, the top of the BL ranged from 500 to 2200 m, with the minimum height generally observed during
25 the morning and gradually increasing during the day, consistent with the increase in heating in the lower troposphere. From the BL structure analyses (communication from D. Lenschow) for the DISCOVER-AQ project, a distinct BuL was present in 80 % of

the profiles (192 of 240). Overall, the AOD contribution from the BL was between 57–61 % (Table 2). Considering the study cases presented in Fig. 4, the BL contribution to the AOD in the usual case (i.e. highly concentrated BL and no aerosol layer aloft similar to 20 July 2011) is about 60 %, while the BuL contribution is lower than 27 %.

5   The presence of an aerosol layer aloft (i.e. similar to 22 or 28 July 2011) dramatically decreases the BL contribution to the AOD (less than 37 %), and thus the extinction from aerosols present in the BuL dominates the AOD (contribution of approximately 60 %). By sorting the data as a function of the presence or the absence of a layer aloft the BL, two distinct tendencies can be observed (Fig. 6). Indeed, when the aerosols are

10 confined in the BL the correlation coefficient between AOD and the $PM_{2.5}$ is relatively high (0.91), and the slope is approximately 74, while the presence of an elevated layer is leading to a spread of the data set (0.71) and a slope 1.6 times lower. Thus, the presence of this layer may lead to an underestimation by a factor of 1.6 of the $PM_{2.5}$ at the surface. These results illustrate the potential pitfall of $PM_{2.5}$ estimation when lofted

15 layers are present.

Figure 7 shows comparisons between AOD derived from the P-3B profiles, the ground-based aerosol mass ($PM_{2.5}$) and aerosol volume measured at the lowest P-3B flight level scaled by $f(RH)_{amb}$ and the height of the surface-coupled, mixed layer. The BL and BuL heights are used to represent the height of this mixed layer. The

20 color code represents the BL and the BL + BuL contribution to the total AOD (Fig. 7a and c, respectively) and highlights the importance of that parameter to retrieve the air quality from the AOD. The $PM_{2.5}$ measurements were limited to 3 out of the 6 ground sites, while the aerosol volume was measured aboard the P-3B over the 6 ground sites and offers thus a more statistically robust comparison (Fig. 7b and d). Moreover, the

25 comparison of the $PM_{2.5}$ with the aerosol volume concentration measured at the lowest level of the P-3B profiles shows high correlation coefficients (0.93, 0.92 and 0.89 respectively at Beltsville, Fairhill, and Edgewood). The slopes of these tendencies correspond to the density of the particles (1.42, 1.2, 1.37 g cm^{-3} respectively at Beltsville, Fairhill, and Edgewood). Strong relationships (with low variability) between column in-

tegrated measurements and the averaged volume of the aerosols sampled in the BL appear as a function of the BL contribution to AOD.

He et al. (2008) have shown that the haze layer concept improves the relationship between $PM_{2.5}$ and the AOD. By integrating Eq. (2) from the surface to the top of the BuL (available from radio soundings), the relationship between the AOD and the $PM_{2.5}$ is strongly improved (R^2>0.95 compare to $R^2 \sim 0.84$ using the BL). The same study has been done using the haze layer calculated from the HSRL measurements (Scarino et al., 2013) and showing similar improvements (Fig. 7c and d, R^2>0.95). Nevertheless, the haze layer is a Lidar product and might not been available for most of the AOD and $PM_{2.5}$ relationship. Thus, this results show that using the BuL instead of the BL from radiosounding measurements will improve the $PM_{2.5}$ retrievals from the AOD.

Few cases show the presence of an aerosol layer above the BuL similar to the case study shown in Fig. 2c. From the profiles of the AOD contribution, the layers above the BuL contribute to more than 10 % of the total AOD, on average. While we show that using the BuL height as the aerosol layer top to be reasonable for the large observational data set obtained in the Baltimore-Washington D.C., there may be other locations where this assumption does not hold. Thus, this study motivates additional work focusing on the relationship between AOD and $PM_{2.5}$ in environments where aerosol layers are frequently observed above the well-defined BL and BuL (e.g. African coast, SE United-States) or in regions with especially shallow BL or BuL heights (e.g., wintertime San Joaquin Valley, California).

The direct comparison of the calculated AOD (Fig. 5) and the measured $PM_{2.5}$ show a strong correlation without taking into account the BL height and f(RH) constrictions due to similar properties of the aerosol sampled within the BL and the BuL. The comparison of the scattering Angstrom exponent (between 450 and 700 nm) and the f(RH) measured during each P-3B profile performed over the DISCOVER-AQ ground sites (Fig. 8) and the average within the BL and the BuL highlights strong similarities of the aerosol physical and chemical properties in each layer. Indeed, more than 72 % of the Angstrom exponents and 88 % of the f(RH) values are within ±10 % of the 1 : 1 line.

Full Screen / Esc

Printer-friendly Version

Interactive Discussion

Very few cases during this campaign show important differences in the aerosol physical or chemical properties. Differences between the BL and BuL aerosol properties might be more frequent over some regions where the atmospheric vertical structure of aerosols is strongly influenced by different aerosol sources.

5.1.2 Relative humidity

High relative humidity conditions, frequently encountered in the BL and in the vicinity of clouds, can result in significant modifications of the optical properties (Twohy et al., 2009; Schuster et al., 2009) due to aerosol hydration. To account for this effect, the frequency of the AOD (calculated from the $\sigma_{ext,amb}$ measured aboard the P-3B or measured by AERONET) at ambient relative humidity as well as water fraction (Eq. 6, Shinozuka et al., 2007) are analyzed (Fig. 9).

$$WF = 1 - \frac{AOD_{dry}}{AOD_{amb}} \tag{6}$$

For most cases ($> 60\%$), the AOD values measured at ambient RH during this campaign were lower than 0.2. Several studies report AOD reference values for remote (Mauna Loa, Hawaii; Holben et al., 2001), rural (Lamont, Oklahoma; Andrews et al., 2011) and urban (Goddard Space Flight Center [GSFC], Maryland; Holben et al., 2001) regions. The AOD observed in the remote atmosphere are below 0.04 all year long (for about 5 yr of measurements), over a rural area values vary between 0.12–0.22 during the summer period (using 7 yr of measurements, 2000–2007) while at GSFC the values were on average 0.45 ± 0.25 for the summer period (using 7 yr of measurements, 1992–1999). The values observed over Washington D.C., - Baltimore, MD area are unusually low during DISCOVER-AQ in summer 2011 and are more representative of rural environment. Comparing the dry and wet AOD highlights the contribution of the aerosol loadings versus the contribution of water uptake and the aerosol loading. The AOD is increasing with the water fraction (Eq. 6), on average from 0.15 for AOD around

0.1 to 0.35 for AOD around 0.35, showing that the larger AOD values (> 0.4) are mainly driven by aerosol water uptake.

During this campaign, the $f(RH)_{amb}$ values were observed to vary significantly from 1.03 to 2.3 on a day-to-day basis, but the profiles were fairly constant within the BL. To isolate the dependence of AOD on aerosol liquid water content effect from the BL contribution, only the cases showing a BL contribution to the AOD larger than 60 % were taken into account. Figure 10 shows the aerosol volume present in the BL sorted as a function of the $f(RH)_{amb}$ averaged in the BL (larger than 1.5 and lower than 1.2) as a function of the $AOD_{P\text{-}3B}$. Slopes for the low $f(RH)_{amb}$ values are twice as high as those for the higher $f(RH)_{amb}$ values (84 versus 40). PM$_{2.5}$ retrievals for AOD = 0.1–0.16 vary by a factor of 1.6 over the range of $f(RH)_{amb}$.

While $f(RH)_{amb}$ vertical profiles are not yet available on a global scale, ground measurements of $f(RH)_{amb}$ or RH are available and can be applied to the entire column to improve the estimation of PM$_{2.5}$ from the AOD. To estimate the errors induced by using the ground measurements, the $f(RH)_{amb}$,ground was calculated using the RH measured at the ground sites and the scattering coefficients (ambient and dry) measured at the lowest level of the P-3B profiles (Fig. 11). Under dry conditions, reasonable agreement (< 10 % error) is observed between the ground-based and P-3B $f(RH)_{amb}$ measurements; however, this agreement worsens considerably at RH > 75 % (errors larger than 19 %). Therefore, in order to estimate the PM$_{2.5}$ from the AOD, the ground $f(RH)_{amb}$ measurements should be used only when the relative humidity throughout the atmospheric column is lower than 55 %.

6   Conclusions

Over 240 profiles of aerosol optical, chemical, and microphysical properties were performed during the NASA DISCOVER-AQ, over Washington D.C., - Baltimore, MD, which offer an excellent opportunity to study the correlation between the air quality observations at the surface and the column integrated measurements. The Aerosol

Optical Depth (AOD) was calculated using the integration of the extinction coefficient measured at 550 nm on board the P-3B throughout the column. The measurements were performed during one month and show that the aerosol mass concentrations ($PM_{2.5}$) measured at the surface (EPA ground sites) are driving the AOD.

Three different atmospheric vertical structures were commonly observed: (i) the aerosol layer is capped by the boundary Layer height (60 % of the profiles), (ii) an aerosol layer capped by the top of the BuL including the BL (17 % of the profiles) and (iii) an aerosol layer disconnected from the BuL and BL (3 % of the profiles). Previous studies (Al-Saadi et al., 2008; Tsai et al., 2011) have discussed the importance of taking into account the aerosol layer height to estimate more precisely the $PM_{2.5}$ from the AOD. The observations show that the variability of the extinction coefficients within the boundary layer (BL) is low (< 9 %) allowing the linear integration over the entire BL altitude range. The contribution of the aerosol present within the BL to the total AOD is used to constrain the relationship between the AOD and $PM_{2.5}$, which highlight different tendency as a function of the presence and the optical thickness of the elevated aerosol layer. Thus, the height of the BL layer combined with the BL contribution improves the $PM_{2.5}$ estimation from AOD. Using the BuL instead of the BL top as the height for the aerosol layer dramatically improves the $PM_{2.5}$ estimation.

The $f(RH)_{amb}$ effect on the estimation of the $PM_{2.5}$ is secondary compared to the BL contribution and induced an error factor of 1.6. Comparision of the observed $f(RH)_{amb,P-3B}$ and the calculated $f(RH)_{amb,ground}$ show that the errors are lower than 10 % when the RH within the BL is lower than 55 % while the errors are larger than 19 % when RH within the BL is larger than 75 %.

This work examines the uncertainties associated with using AOD measurements to estimate ground-based $PM_{2.5}$, and finds that accurate quantification of the aerosol mixed-layer height is paramount for accurately predicting $PM_{2.5}$ concentrations, while capturing the compositional-based $f(RH)_{amb}$ variability shows a less-pronounced improvement. The generally dry conditions observed throughout the study may partially explain why $f(RH)$ variability is found to be a second-order effect in the overall esti-

mates, and suggests a much greater uncertainty under predominantly humid conditions (as shown in Fig. 10). Since these results are representative of unseasonably dry conditions in the Baltimore-Washington metropolitan area, extrapolating these results to other geographical locations must be done with care. The four field campaigns planned during the DISCOVER-AQ project offer an opportunity to perform similar studies over different regions characterized by a wide variety of aerosol sources and meteorological conditions. Together these studies will provide a better understanding of the ability of future remote-sensing retrievals to quantify surface $PM_{2.5}$ on a global or regional scale.

References

Al-Saadi, J., Soja, A., Pierce, R. B., Szykman, J., Wiedinmyer, C., Emmons, L., Kondragunta, S., Zhang, X., Kittaka, C., Schaack, T., and Bowman, K.: Intercomparison of near-real-time biomass burning emissions estimates constrained by satellite fire data, J. Appl. Remote Sens., 2, 021504, doi:10.1117/1.2948785, 2008.

Annesi-Maesano, I., Forastiere, F., Kunzli, N., and Brunekref, B.: Particulate matter, science and EU policy, European Respiratory Journal, 29, 428–431, 2007.

Beyersdorf, A. J., Chen, G., Crumeyrolle, S., Thornhill, K. L., Winstead, E., Ziemba, L. D., and Anderson, B. E.: Aerosol Composition and Variability in the Baltimore-Washington D.C. Region, in preparation, 2013.

Anderson, T. L. and Ogren, J. A.: Determining aerosol radiative properties using the TSI 3563 integrating nephelometer, Aerosol Sci. Technol., 29, 57–69, 1998.

Andrews, E., Sheridan, P. J., Ogren, J. A., and Ferrare, R.: In Situ Aerosol Profiles over the Southern Great Plains CART site, Part I: Aerosol Optical Properties, J. Geophys. Res., 109, D06208, doi:10.1029/2003JD004025, 2004.

Andrews, E., Sheridan, P. J., and Ogren, J. A.: Seasonal differences in the vertical profiles of aerosol optical properties over rural Oklahoma, Atmos. Chem. Phys., 11, 10661–10676, doi:10.5194/acp-11-10661-2011, 2011.

Chu, D. A., Kaufman, Y. J., Zibordi, G., Chern, J. D., Mao, J., Li, C., and Holben, B. N.: Global monitoring of air pollution over land from the Earth Observing System-Terra Moderate Resolution Imaging Spectroradiometer (MODIS), J. Geophys. Res., 108, 4661, doi:10.1029/2002JD003179, 2003.

Collaud Coen, M., Andrews, E., Asmi, A., Baltensperger, U., Bukowiecki, N., Day, D., Fiebig, M., Fjaeraa, A. M., Flentje, H., Hyvärinen, A., Jefferson, A., Jennings, S. G., Kouvarakis, G., Lihavainen, H., Lund Myhre, C., Malm, W. C., Mihapopoulos, N., Molenar, J. V., O'Dowd, C., Ogren, J. A., Schichtel, B. A., Sheridan, P., Virkkula, A., Weingartner, E., Weller, R., and Laj, P.: Aerosol decadal trends – Part 1: In-situ optical measurements at GAW and IMPROVE stations, Atmos. Chem. Phys., 13, 869–894, doi:10.5194/acp-13-869-2013, 2013.

Draxler, R. R. and Rolph, G. D.: HYSPLIT (HYbrid Single-Particle Lagrangian Integrated Trajectory), Model access via NOAA ARL READY Website (http://ready.arl.noaa.gov/HYSPLIT.php), NOAA Air Resources Laboratory, Silver Spring, MD, 2010.

Engel-Cox, J. A., Holloman, C. H., Coutant, B. W., and Hoff, R. M.: Qualitative and quantitative evaluation of MODIS satellite sensor data for regional and urban scale air quality, Atmos. Environ., 38, 2495–2509, doi:10.1016/j.atmosenv.2004.01.039, 2004.

Engel-Cox, J. A., Hoff, R. M., Rogers, R., Dimmick, F., Rush, A. C., Szykman, J. J., Al-Saadi, J., Chu, D. A., and Zell, E. R.: Integrating LIDAR and satellite optical depth with ambient monitoring for 3-D dimensional particulate characterisation, Atmos. Environ., 40, 8056–8067, 2006.

Feczkó, T., Molnár, A., Mészáros, E., and Major, G.: Regional climate forcing of aerosol estimated bya a box model for a rural site in Central Europe during summer, Atmos. Environ., 36, 4125–4131, 2002.

Gao, R. S., Ballard, J., Watts, L. A., Thornberry, T. D., Ciciora, S. J., McLaughlin, R. J., and Fahey, D. W.: A compact, fast UV photometer for measurement of ozone from research aircraft, Atmos. Meas. Tech., 5, 2201–2210, doi:10.5194/amt-5-2201-2012, 2012.

PM$_{2.5}$ values inferred from satellite observations

S. Crumeyrolle et al.

Title Page

Abstract | Introduction

Conclusions | References

Tables | Figures

Back | Close

Full Screen / Esc

Printer-friendly Version

Interactive Discussion

Gupta, P. and Christopher, S. A.: Particulate matter air quality assessment using integrated surface, satellite, and meteorological products: Multiple regression approach, J. Geophys. Res., 114, D14205, doi:10.1029/2008JD011496, 2009a.

Gupta, P. and Christopher, S. A.: Particulate matter air quality assessment using integrated surface, satellite, and meteorological products: 2. A neural network approach, J. Geophys. Res., 114, D20205, doi:10.1029/2008JD011497, 2009b.

Gupta, P., Christopher, S. A., Wang, J., Gehrig, R., Lee, Y., and Kumar, N.: Satellite remote sensing of particulate matter and air quality assessment over global cities, Atmos. Environ., 40, 5880–5892, 2006.

Gupta, P., Christopher, S. A., Box, M. A., and Box, G. P.: Multi year satellite remote sensing of particulate matter air quality over Sydney, Australia, Int. J. Rem. Sens., 28, 4483–4498, 2007.

Hartley, W. S., Hobbs, P. V., Ross, J. L., Russell, P. B., and Livingston, J. M.: Properties of aerosols aloft relevant to direct radiative forcing off the mid-Atlantic coast of the United States, J. Geophys. Res., 105, 9859–9885, 2000.

He, Q., Li, C., Mao, J., Lau, A. K.-H., and Chu, D. A.: Analysis of aerosol vertical distribution and variability in Hong Kong, J. Geophys. Res., 113, D14211, doi:10.1029/2008JD009778, 2008.

Hoff, R. M. and Christopher, S. A.: Remote sensing of Particulate Pollution from Space: Have we reached the Promised Land?, J. Air Waste Manage. Assoc., 59, 645–675, doi:10.3155/1047-3289.59.6.645, 2009.

Holben, B. N., Eck, T. F., Slutsker, I., Tanré, D., Buis, J. P., Setzer, A., Vermote, E., Reagan, J. A., Kaufman, Y., Nakajima, T., Lavenu, F., Jankowiak, I., and Smirnov, A.: AERONET–A Federated Instrument Network and Data Archive for Aerosol Characterization, Remote Sens. Environ., 66, 1–16, 1998.

Holben, B. N., Tanre, D., Smirnov, A., Eck, T. F., Slutsker, I., Abuhassan, N., Newcomb, W. W., Schafer, J., Chatenet, B., Lavenue, F., Kaufman, Y. J., Vande Castle, J., Setzer, A., Markham, B., Clark, D., Frouin, R., Halthore, R., Karnieli, A., O'Neill, N. T., Pietras, C., Pinker, R. T., Voss, K., and Zibordi, G.: An emerging ground-based aerosol climatology: Aerosol Optical Depth from AERONET, J. Geophys. Res., 106, 12067–12097, 2001.

Koelemeijer, R. B. A., Homan, C. D., and Matthijsen, J.: Comparison of spatial and temporal variations of aerosol optical thickness and particulate matter over Europe, Atmos. Environ., 40, 5304–5315, 2006.

Title Page

Abstract | Introduction

Conclusions | References

Tables | Figures

|◄ | ►|

◄ | ►

Back | Close

Full Screen / Esc

Printer-friendly Version

Interactive Discussion

Kumar, N., Chu, A., and Foster, A.: An empirical relationship between $PM_{2.5}$ and aerosol optical depth in Delhi Metropolitan, Atmos. Environ., 41, 4492–4503, 2007.

Kumar, N., Chu, A., and Foster, A.: Remote sensing of ambient particles in Delhi and its environs: Estimation and validation, Int. J. Remote Sens., 29, 3383–3405, 2008.

Lenschow, D. H., Krummel, P. B., and Siems, S. T.: Measuring entrainment, divergence and vorticity on the mesoscale from an aircraft, J. Atmos. Ocean. Technol., 16, 1384–1400, 1999.

Liu, Y., Sarnat, J. A., Kilaru, V., Jacob, D. J., and Koutrakis, P.: Estimating Ground Level $PM_{2.5}$ in the Eastern United States Using Satellite Remote Sensing, Environ. Sci. Technol., 3, 3269–3278, 2005.

Macias, E. S. and Husar, R. B.: Atmospheric particulate mass measurement with beta attenuation mass monitor, Environ. Sci. Technol., 10, 904–907, 1976.

McNaughton, C. S., Clarke, A. D., Howell, S. G., Pinkerton, M., Anderson, B. E., Thornhill, L., Hudgins, C., Winstead, E., Dibb, J. E., Scheuer, E., and Maring, H.: Results from the DC-8 Inlet Characterization Experiment (DICE): Airborne versus surface sampling of mineral dust and sea salt aerosols, Aerosol Sci. Technol., 41, 136–159, doi:10.1080/02786820601118406, 2007.

Peltier, R. E., Sullivan, A. P., Weber, R. J., Brock, C. A., Wollny, A. G., Holloway, J. S., de Gouw, J. A., and Warneke, C.: Fine aerosol bulk composition measured on WP-3D research aircraft in vicinity of the Northeastern United States – results from NEAQS, Atmos. Chem. Phys., 7, 3231–3247, doi:10.5194/acp-7-3231-2007, 2007.

Pereira, S., Wagner, F., and Silva, A. M.: Scattering properties and mass concentration of local and long range transported aerosols over the south western Iberian Peninsula, Atmos. Environ., 42, 7623–7631, 2008.

Pilinis, C. and J. Seinfeld. Water content of atmospheric aerosols, Atmos. Environ., 23, 1601–1606, 1989.

Russell, L. M., Lenschow, D. H., Laursen, K. K., Krummel, P. B., Siems, S. T., Bandy, A. R., Thornton, D. C., and Bates, T. S.: Bidirectional mixing in an ace 1 marine boundary layer overlain by a second turbulent layer, J. Geophys. Res., 103, 16411–16432, 1998.

Ryder, C. L., Highwood, E. J., Rosenberg, P. D., Trembath, J., Brooke, J. K., Bart, M., Dean, A., Crosier, J., Dorsey, J., Brindley, H., Banks, J., Marsham, J. H., McQuaid, J. B., Sodemann, H., and Washington, R.: Optical properties of Saharan dust aerosol and contribution from the coarse mode as measured during the Fennec 2011 aircraft campaign, Atmos. Chem. Phys., 13, 303–325, doi:10.5194/acp-13-303-2013, 2013.

PM$_{2.5}$ values inferred from satellite observations

S. Crumeyrolle et al.

Title Page

Abstract | Introduction

Conclusions | References

Tables | Figures

◀ | ▶

◀ | ▶

Back | Close

Full Screen / Esc

Printer-friendly Version

Interactive Discussion

Scarino, A. J., Obland, M. D., Fast, J. D., Burton, S. P., Ferrare, R. A., Hostetler, C. A., Berg, L. K., Lefer, B., Haman, C., Hair, J. W., Rogers, R. R., Butler, C., Cook, A. L., and Harper, D. B.: Comparison of mixed layer heights from airborne high spectral resolution lidar, ground-based measurements, and the WRF-Chem model during CalNex and CARES, Atmos. Chem. Phys. Discuss., 13, 13721–13772, doi:10.5194/acpd-13-13721-2013, 2013.

Schaap, M., Apituley, A., Timmermans, R. M. A., Koelemeijer, R. B. A., and de Leeuw, G.: Exploring the relation between aerosol optical depth and $PM_{2.5}$ at Cabauw, the Netherlands, Atmos. Chem. Phys., 9, 909–925, doi:10.5194/acp-9-909-2009, 2009.

Schafer, K., Harbusch, A., Emeis, S., Koepke, P., and Wiegner, M.: Correlation of aerosol mass near the ground with aerosol optical depth during two seasons in Munich, Atmos. Environ., 42, 4036–4046, 2008.

Schmid, B., Livingston, J. M., Russell, P. B., Durkee, P. A., Jonsson, H. H., Collins, D. R., Flagan, R. C., Seinfeld, J. H., Gassó, S., Hegg, D. A., Öström, E., Noone, K. J., Welton, E. J., Voss, K. J., Gordon, H. R., Formenti, P., and Andreae, M. O.: Clear-sky closure studies of lower tropospheric aerosol and water vapor during ACE-2 using sunphotometer, airborne in-situ, space-borne and ground-based measurements, Tellus B, 52, 568–593, 2000.

Schmid, B., Flynn, C. J., Newsom, R. K., Turner, D. D., Ferrare, R. A., Clayton, M. F., Andrews, E., Ogren, J. A., Johnson, R. R., Russell, P. B., Gore, W. J., and Dominguez, R.: Validation of aerosol extinction and water vapor profiles from routine Atmospheric Radiation Measurement Climate Research Facility measurements, J. Geophys. Res., 114, D22207, doi:10.1029/2009JD012682, 2009.

Schuster, G. L., Lin, B., and Dubovik, O.: Remote sensing of aerosol water uptake, Geophys. Res. Lett., 36, L03814, doi:10.1029/2008gl036576, 2009.

Sheridan, P. J., Jefferson, A., and Ogren, J. A.: Spatial variability of submicrometer aerosol radiative properties over the Indian Ocean during INDOEX, J. Geophys. Res., 107, 8011, doi:10.1029/2000JD000166, 2002.

Shinozuka, Y., Clarke, A. D., Howell, S. G., Kapustin, V. N., McNaughton, C. S., Zhou, J., and Anderson, B. E.: Aircraft profiles of aerosol microphysics and optical properties over North America: Aerosol optical depth and its association with PM2.5 and water uptake, J. Geophys. Res., 112, D12S20, doi:10.1029/2006JD007918, 2007.

Tian, J. and Chen, D. M.: Spectral, spatial, and temporal sensitivity of correlating MODIS aerosol optical depth with ground-based fine particulate matter ($PM_{2.5}$) across southern Ontario, Can. J. Remote Sens., 36, 119–128, 2010.

Title Page

Abstract | Introduction

Conclusions | References

Tables | Figures

|◄ | ►|

◄ | ►

Back | Close

Full Screen / Esc

Printer-friendly Version

Interactive Discussion

Tsai, T. C., Jeng, Y. J., Chu, D. A., Chen, J. P., Chang, S. C.: Analysis of the relationship between MODIS aerosol optical depth and particulate matter from 2006 to 2008, Atmos. Environ., 45, 4777–4788, 2011.

Twohy, C. H., Coakley, J. A., and Tahnk, W. R.: Effect of changes in relative humidity on aerosol scattering near clouds, J. Geophys. Res., 114, doi:10.1029/2008JD010991, 2009.

Van Donkelaar, A., Martin, R. V., and Park, R. J.: Estimating groundlevel $PM_{2.5}$ using aerosol optical depth determined from satellite remote sensing, J. Geophys. Res., 111, D21201, doi:10.1029/2005JD006996, 2006.

Vidot, J., Santer, R., and Ramon, D.: Atmospheric particulate matter (PM) estimation from SeaWIFS imagery, Remote Sens. Environ., 111, 1–10, 2007.

Virkkula, A.: Correction of the Calibration of the 3-wavelength Particle Soot Absorption Photometer (3 PSAP), Aerosol Sci. Technol., 44, 706–712, doi:10.1080/02786826.2010.482110, 2010.

Volkamer, R., Jimenez, J. L., San Martini, F., Dzepina, K., Zhang, Q., Salcedo, D., Molina, L. T., Worsnop, D. R., and Molina, M. J.: Secondary organic aerosol formation from anthropogenic air pollution : Rapid and higher than expected, Geophys. Res. Lett., 33, L17811, doi:10.1029/2006GL026899, 2006.

Wang, J. and Christopher, S. A.: Intercomparison between satellite derived aerosol optical thickness and $PM_{2.5}$ mass: Implications for air quality studies, Geophys. Res. Lett., 30, 2095, doi:10.1029/2003GL018174, 2003.

Zhang, R., Khalizov, A. F., Pagels, J., Zhang, D., Xue, H., and McMurry, P. H.: Variability in morphology, hygroscopicity, and optical properties of soot aerosols during atmospheric processing, P. Natl. Acad. Sci., 105, 10291–10296, doi:10.1073/pnas.0804860105, 2008.

Ziemba, L., Thornhill, K., Ferrare, R., Barrick, J., Beyersdorf, A., Chen, G., Crumeyrolle, S., Hair, J., Hostetler, C., Hudgins, C., Obland, M., Rogers, R., Scarino, A., Winstead, E., and Anderson, B. E.: Airborne observations of aerosol extinction by in-situ and remote-sensing techniques: Evaluation of particle hygroscopicity, Geophys. Res. Lett., 40, 417–422, 2013.

Ziemba, L. D., Fischer, E., Griffin, R. J., and Talbot, R. W.: Aerosol acidity in rural New England: Temporal trends and source region analysis, J. Geophys. Res.-Atmos., 112, doi:10.1029/2006JD007605, 2007.

Table 1. Aerosol Optical Depth calculated for the study cases shown in Fig. 3a, b and c for ethe boundary layer (BL), theBuffer Layer (BuL) and the free troposphere above the BuL (FT). The AOD contribution are indicated in the parenthesis.

	Case 1 (Fig. 3a)	Case 2 (Fig. 3b)	Case 3 (Fig. 3c)
AOD$_{BL}$	0.23 (62 %)	0.17 (46 %)	0.05 (16 %)
AOD$_{BuL}$	0.14 (38 %)	0.18 (48 %)	0.14 (47 %)
AOD$_{FT}$	0.00 (0 %)	0.02 (5 %)	0.11 (37 %)

Table 2. The lower 10th, median and 90th percentile values of the boundary layer and the buffer layer (when it exist) contribution to the total AOD (%). The sample number is size is given under "N".

Ground site	Boundary Layer (BL)				Buffer Layer (BuL)			
	N	10th	Med	90th	N	10th	Med	90th
Beltsville	–	–	–	–	–	–	–	–
Fairhill	29	42	61	80	25	11	27	42
Edgewood	32	36	57	78	29	12	32	51
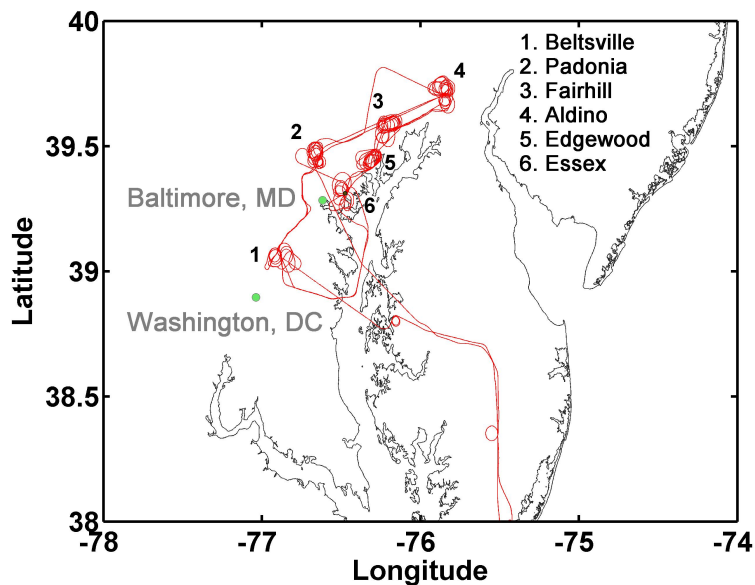
Fig. 1. Location of the DISCOVER-AQ field campaign #1 over Washington, D.C. – Baltimore, MD area. The flight path followed by the P-3B is represented by the red line and the numbers correspond to the ground sites. Flight paths did not vary greatly between flights.
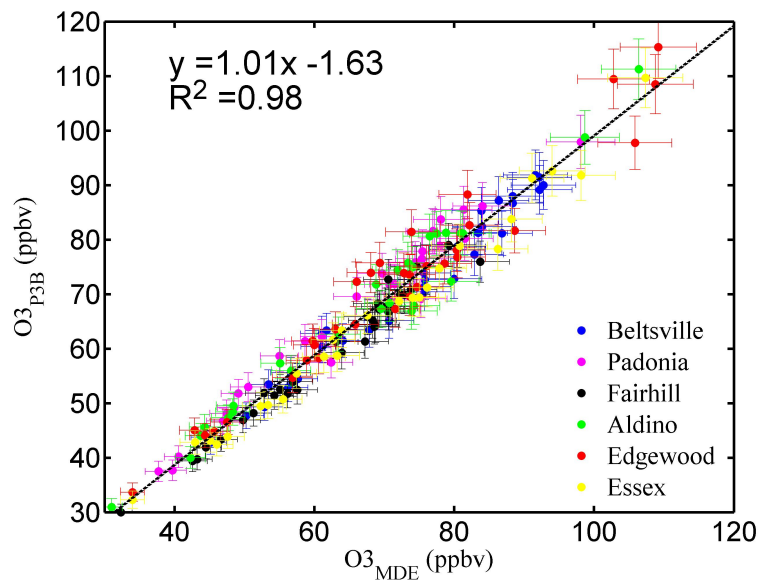
Fig. 2. Ozone measured from the EPA ground sites (at Beltsville, Padonia, Fairhill, Aldino, Edgewood and Essex) as a function of the ozone measured on-board the P-3B at the lowest level of each profile.
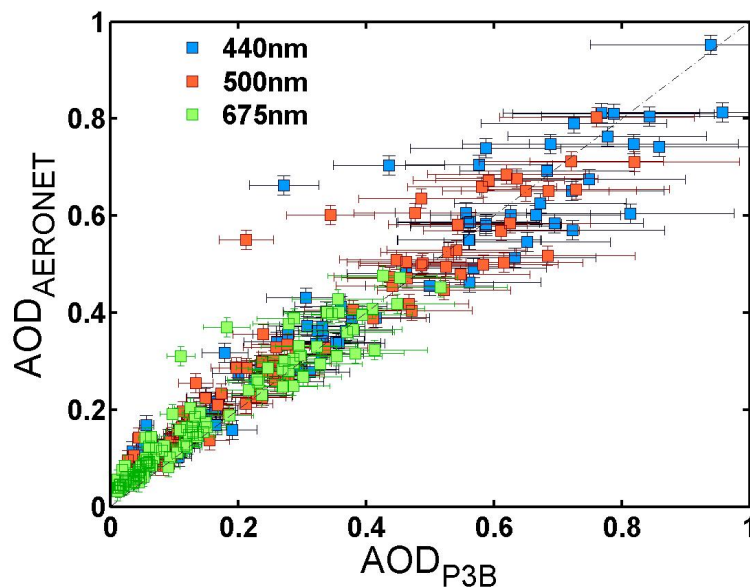
Fig. 3. AOD measured by AERONET as a function of AOD retrieved from the P-3B extinction measurements for three wavelengths (440, 500 and 675 nm, respectively blue, green and red). The error bar depicts the instrumental variability for the AOD calculated from the P-3B measurements and ±0.02 for the AOD measured by AERONET (Holben et al., 1998).
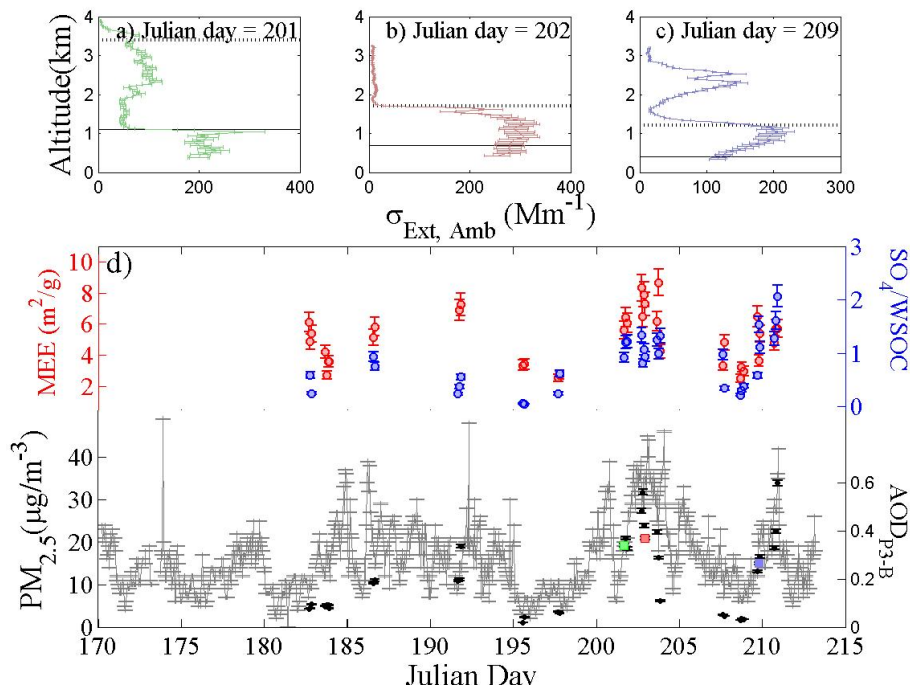
Fig. 4. Profiles **(a, b, c)** of the ambient extinction coefficient observed aboard the P-3B over Edgewood on 20, 21 and 28 July 2011 respectively. Time series **(d)** of the aerosol optical depth (AOD, black dots) calculated from the integration over the column of the extinction coefficients measured aboard the P-3B, the PM$_{2.5}$ measured from the Edgewood ground site (grey line), the mass extinction efficiency (MEE, red dots) and the ratio of the sulphate mass concentration over the water soluble organic mass concentration (blue dots) measured at the lowest level of the P-3B profiles.
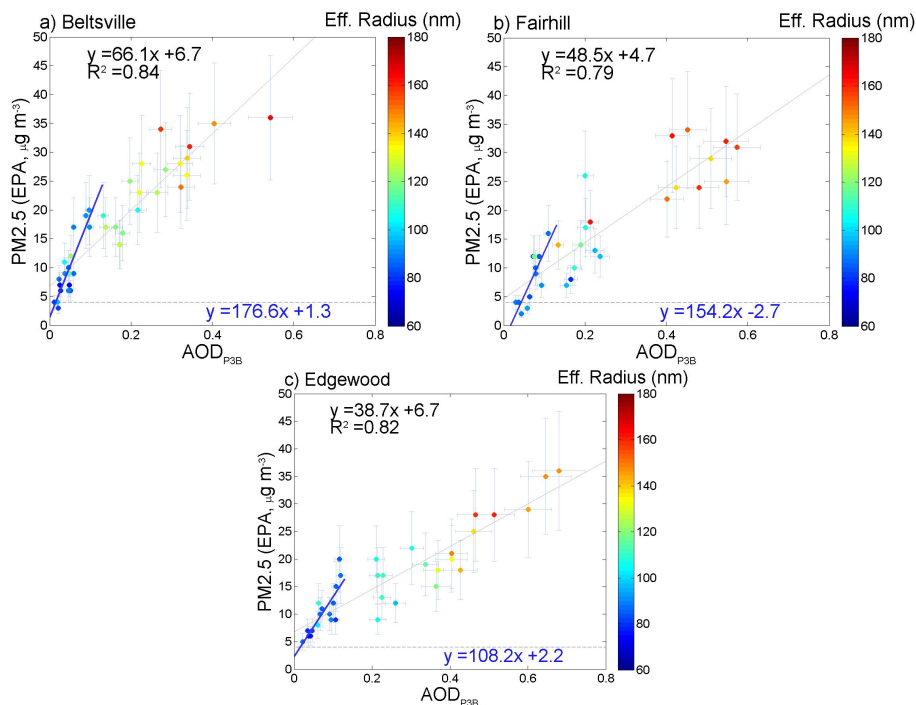
Fig. 5. PM$_{2.5}$ measured from the EPA ground sites (at Beltsville **a**, Fairhill **b**, and Edgewood **c**) as a function of the AOD calculated using extinction profiles performed by the P-3B. The color code represents the effective radius (nm). The horizontal dashed line corresponds to the detection limit of the BAM (4 µg m^{-3}). The error bars correspond to the measurement variability (±1σ).

The chart shows:
- Legend: Well Mixed (black dots), Layer aloft (red squares)
- Y-axis: PM2.5 (EPA, μgm^{-3})
- X-axis: AOD (P3B)
- $y = 74x - 3.9$, $R^2 = 0.91$
- $y = 46.3x - 6.41$, $R^2 = 0.71$
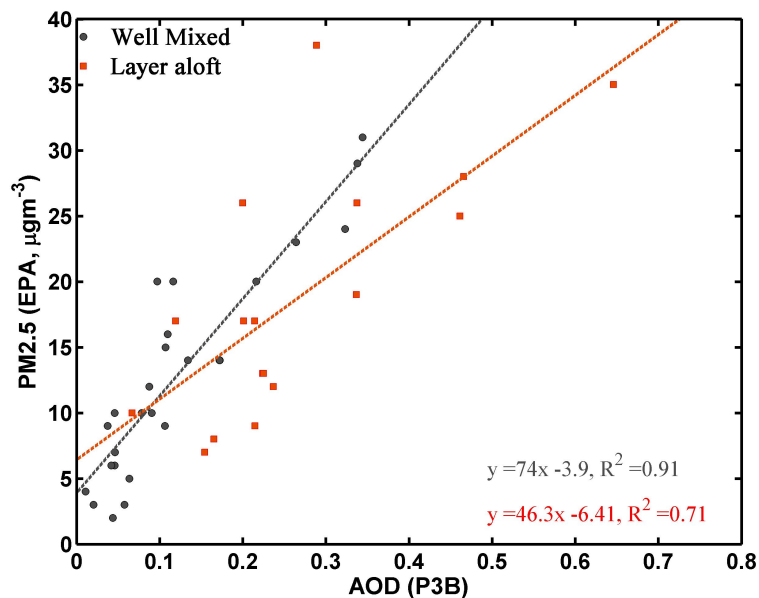
Fig. 6. Also shown are correlation plots of the dry extinction as a function of the PM$_{2.5}$ measured from the EPA ground sites **(d)** at Beltsville, **(e)** at Fairhill, and **(f)** at Edgewood, color-coded by the effective radius. The vertical dashed line corresponds to the detection limit of the BAM (4 μg m^{-3}). The error bars correspond to the measurement variability ($\pm 1\sigma$).

Title Page

Abstract | Introduction

Conclusions | References

Tables | Figures

|◀ | ▶|

◀ | ▶

Back | Close

Full Screen / Esc

Printer-friendly Version

Interactive Discussion
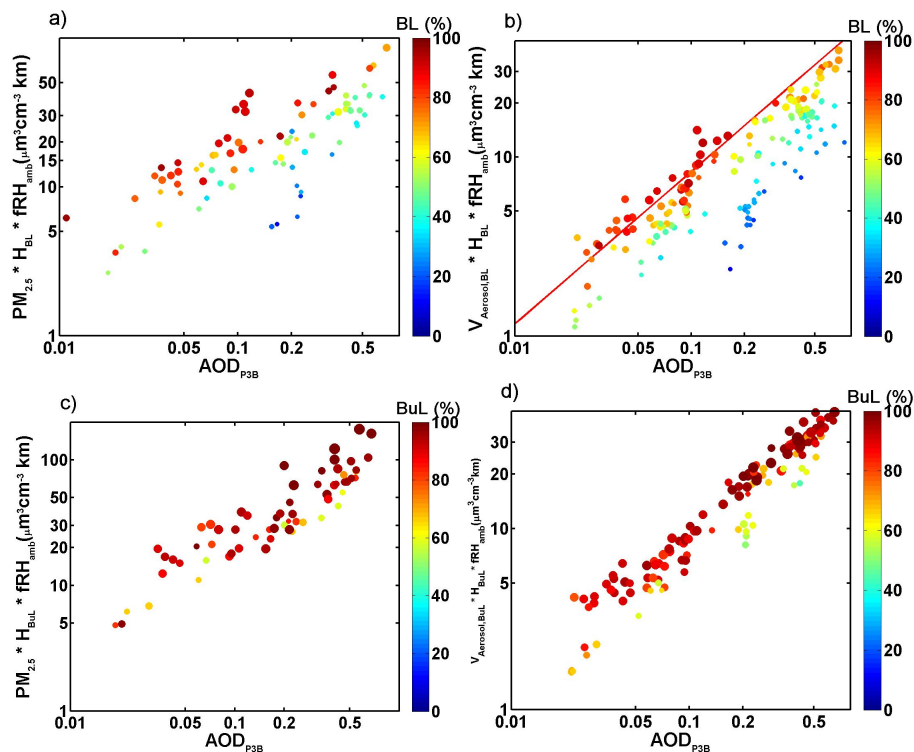
Fig. 7. Ambient AOD measured by the P-3B as a function of the Volume concentration weighted by the BL height and the $f(\mathrm{RH})_{amb}$. The color code represents the BL contribution to the AOD and the size of each dot correspond to the BL height. The red line is coresponding to the linear fit of cases where the the AOD contribution of the BL is higher than 75 %.

Title Page

Abstract · Introduction

Conclusions · References

Tables · Figures

|◄ · ►|

◄ · ►

Back · Close

Full Screen / Esc

Printer-friendly Version

Interactive Discussion
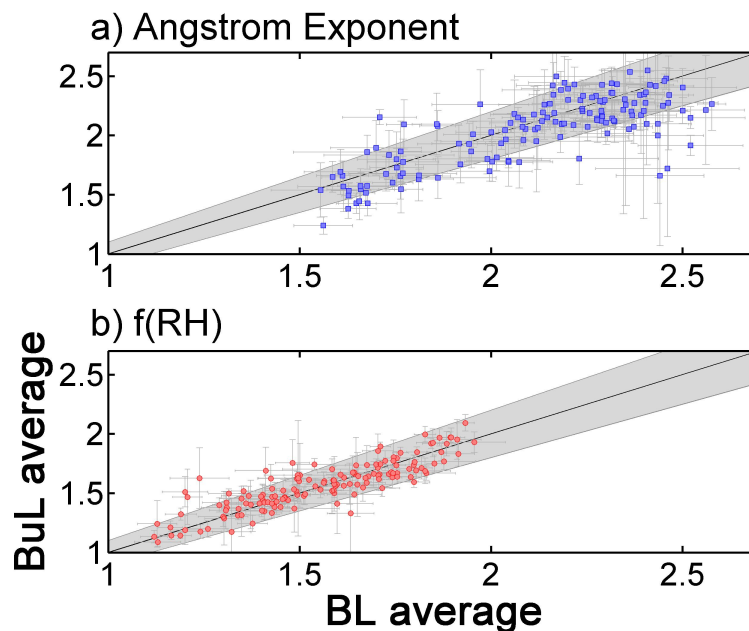
Fig. 8. Comparison of the Angstrom exponent between 450 and 700 nm **(a)**, and the f(RH) **(b)** averaged within the BL (Boundary Layer) and the BuL (Buffer Layer) at the different DISCOVER-AQ sites (Beltsville, Padonia, Fairhill, Aldino, Edgewood and Essex). The black line corresponds to the 1 : 1 line and the gray area represents the 10 % variability.
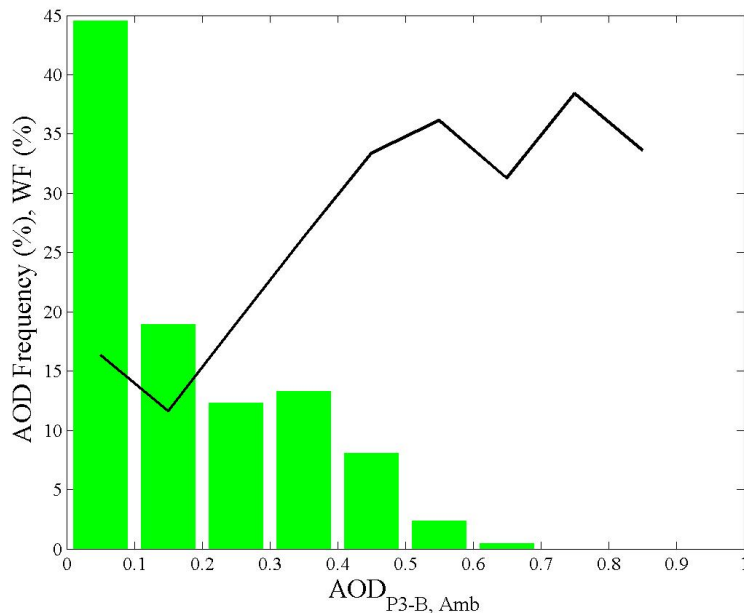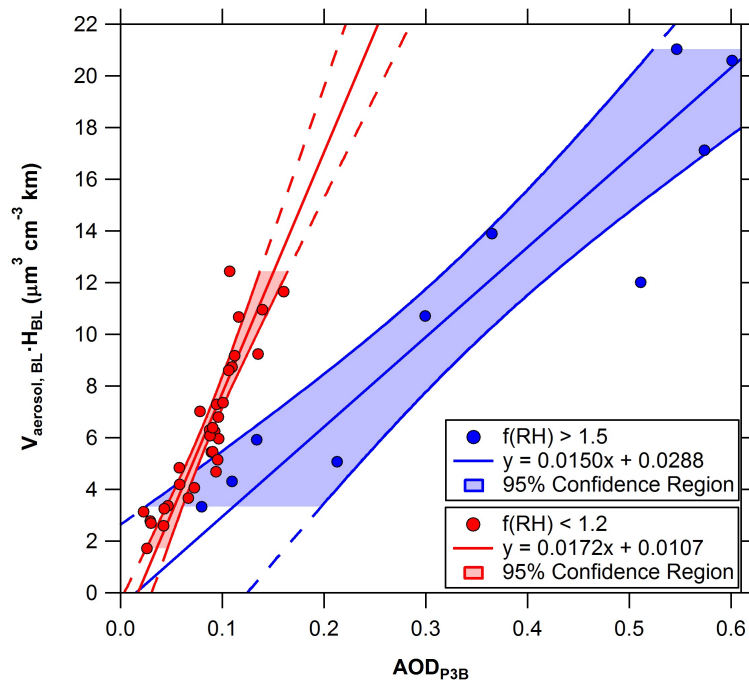
Fig. 9. Frequency of the AOD retrieved from ambient extinction coefficient measured aboard the P-3B and the water fraction (WF, %) associated with observed dry (P-3B) and ambient (P-3B) AOD.

Fig. 10. Aerosol volume concentration averaged in the BL weighted by the BL height, when the aerosols present in the BL are contributing at 60 % and more, as a function of the AOD from the P-3B measurements. The red (blue) color correspond to $f(RH)_{amb}$ values lower (larger) than 1.2 (1.5).

Full Screen / Esc

Printer-friendly Version

Interactive Discussion
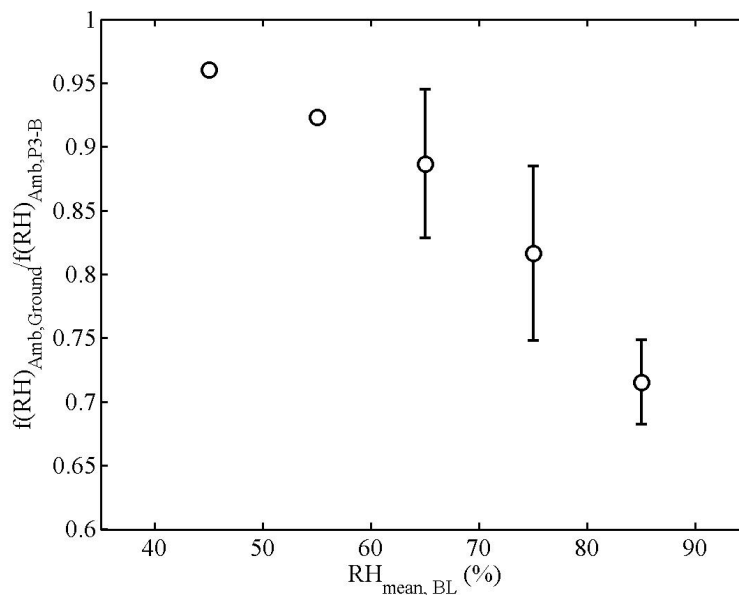
Fig. 11. Ratio of the $f(RH)_{amb,ground}$ to $f(RH)_{amb,P-3B}$ as a function of the averaged relative humidity measured during the P-3B profiles within the BL.